Effects of fixation and preservation on tissue elastic properties measured by quantitative optical coherence elastography (OCE)

Ling, Yuting; Li, Chunhui; Feng, Kairui; Duncan, Robyn; Eisma, Roos ; Huang, Zhihong

Published in:
Journal of Biomechanics

DOI:
10.1016/j.jbiomech.2016.02.013

Publication date:
2016

Document Version
Peer reviewed version

Effects of fixation and preservation on tissue elastic properties measured by quantitative optical coherence elastography (OCE)

Yuting Ling[1, 2, ǂ], Chunhui Li[1, 2, ǂ], Kairui Feng[2], Robyn Duncan[3], Roos Eisma[3], Zhihong Huang[2], Ghulam Nabi[1]

[1]*Academic Section of Urology, Division of Imaging Technology, School of Medicine, University of Dundee, Dundee DD1 9SY, Scotland, UK*

[2]*School of Engineering, Physics and Mathematics, University of Dundee, Dundee DD1 4HN, Scotland, UK*

[3]*Centers for Anatomy and Human Identification, College of Life Sciences, University of Dundee, Dundee, UK, DD1 4HN*

ǂ: These authors contribute equally in this work

Abstract

Fixed and preserved tissues have been massively used in the development of biomedical equipment and instrumentation. Not only the tissue morphology, but also its mechanical properties need to be considered in the fixation and preservation procedures since mechanical properties have significant influence on the design and performance of such instruments. Understanding the effects of storage and preservation conditions on the mechanical properties of soft tissue has both clinical and experimental significance. To this end, we aimed to study the effects of tissue preservation (by 10% formalin and Thiel fluids) on the elastic properties of five different kinds of fresh tissues from pig and chicken; specifically fat, liver, muscle, tendon and cartilage. The tissue elasticity was measured intensively and strictly within a controlled timeline of 6 months by quantitative optical coherence elastography (OCE) system. Our findings suggest that the elasticity change of tissues in the formalin solution has an ascending trend, but that of Thiel remains almost constant, providing a more real texture and properties.

Keywords: Soft tissue; Optical coherence elastography (OCE); Fixation; Formalin solution; Thiel fluids; Elastic properties.

1. Introduction

Fixation and preservation of tissue is a crucial step in preparation specimens for microscopic histopathological examination. In addition to stopping tissue from degrading, fixation offers easier handling, prolonged storage and precise sectioning of tissues to uniform morphology. Aldehydes have the property of crosslinking by creating covalent chemical bonds between proteins (Abe et al., 2003). Soluble proteins are fixed

to structural proteins and are rendered insoluble and the whole structure is given mechanical strength. Aldehyde fixation has direct influence on tissue mechanical properties by forming an increased number of inter- and intra-fibrillar cross-links of primary amine groups of polypeptide chains (Currey et al., 1995; Boskey et al. 1982). The most popular fixing agent is formaldehyde (CH_2O). A saturated water solution (37% – 40% w/v) is formed by dissolving the gaseous formaldehyde in water, which is called '100% formalin'. A small amount of methanol is usually added as a stabilizer to prevent oxidation and polymerization. For fixation, an optimal concentration is 10% formalin solution containing 4% formaldehyde w/v. 4% formalin solution is produced by diluting one part formalin with nine parts of water or buffer. One day's fixation period is commonly required in most applications since it is believed that the main process of formaldehyde fixation is finished within 24 hours. The volume of the formalin solution required depends on the size and thickness of tissues (Buesa and Peshkov, 2012).

Formaldehyde is considered dangerous and toxic and as a result concerns have been raised about the potential health risks of traditional formalin embalming techniques (Eisma et al. 2013). Thiel embalming is a new soft-fix embalming technique. The embalming procedure consists of an initial perfusion followed by immersion in thiel fluid for at least 2 months (Eisma et al., 2013). The main components are water, glycol and salts. The solutions comprise of very low concentrations of harmful components: formaldehyde, chlorocresol and morpholine. Due to the high concentration of salt components, proteins in the tissues are denatured, leading to a homogenization of the tissues (Wolff et al. 2008). The Thiel embalming method has been developed and refined over the last three decades in Graz, Austria and is currently utilised by the Centre for Anatomy and Human Identification (CAHiD) at the University of Dundee (Eisma et al., 2013; Thiel, 2002). According to recent reports (Eisma et al., 2013; Buesa and Peshkov, 2012), Thiel embalming can provide long-lasting preservation with impressive flexibility and tissue quality, especially for the application in microvascular exercise and other surgical and clinical training.

In addition to the successful application on histopathology, fixed and preserved tissue is also served as a useful tool for clinical training and biomedical instrumentation design (McLeod et al., 2010; Eljamel et al. 2014). In this case it is not only the tissue morphology that need to be considered but also its mechanical properties since they have significant influence to the design and performance of such instruments. Fixation

induced mechanical property changes have attracted attention and studies have been carried out to investigate the effects of tissue preservation methods on the mechanical properties of different kinds of tissues using traditional mechanical loading methods (McLeod et al., 2010; Eljamel et al. 2014; McElhaney et al. 1964; Sedlin, 1965; Goh and Ang, 1989; Tan et al., 2002; Kikugawa and Asaka, 2005). However, to the best of our knowledge there are some limitations regarding to the current studies of the fixation effects to mechanical properties of tissue: 1) the traditional loading method cannot provide real time elasticity change since it is a relatively time consuming technique, thus the detailed elasticity change with precise time line during the fixation procedure cannot be determined; 2) the degree of influence of different fixation methods to mechanical properties in relation to different kinds of tissues remains unknown.

Optical Coherence Tomography (OCT) is an optical imaging technique that enables high-resolution, cross-sectional imaging of tissue microstructures, *in vivo*, non-invasive and in real time (Fercher, 2010; Tomlins and Wang, 2005; Welzel, 2001; Sun et al., 2011; Schmitt, 1998; Chan et al., 2004; Rogowska, 2004; Ko et al., 2006; Wang et al., 2006; Kirkpatric et al., 2006; Liang et al., 2008; Wang et al., 2007; Kennedy et al., 2009; Kennedy et al., 2011; Tearney et al., 1997; D'Amico et al., 2000). Optical Coherence Elastography (OCE) has become increasingly utilised as it carries the potential to provide ultra-high resolution imaging which not only has the ability to detect subtle changes in material structure but also can characterise materials based on their mechanical properties (stiffness). The basic concept of OCE is to stimulate vibration in the target tissue and measure the vibration amplitude corresponding to strain. Areas with higher vibrating amplitude indicate a softer material while areas with lower vibrating amplitude indicate a stiffer material (Kennedy et al., 2009; Kennedy et al., 2011; Guan et al., 2013). Compared with other elastography methods, i.e. ultrasound and magnetic resonance elastography, OCE is capable of providing ultra-high microstructural and mechanical characterization, and therefore has the potential to resolve the microscopic heterogeneity in the assessment of mechanical properties of tissues. OCE also has high acquisition speed with 2D image acquisition rates in the range of 10s to 100s of kHz, and potentially even higher, which has great potential to fulfil real time 2D elastography. OCE has high mechanical sensitivity which enables displacement detection up to picometers (Wang et al. 2010). It has the potential to improve differentiations between small alterations in mechanical properties. Recent

work using a novel quantitative OCE method has shown promising results (Li et al., 2014). The mechanical properties of tissue were estimated using OCE while providing the ultra-high resolution with elastography of OCT images. Building on this technological advance and experience enables the use of 3D quantitative OCE imaging using a spectral-domain OCT (SD-OCT) system combined with an electromagnetic actuator.

This paper explores the use of quantitative OCE to provide quantitative mechanical property changes induced by fixation procedure. To achieve this goal, the elasticity changes of five different kinds of tissue were compared under the fixation of 10% diluted formalin and Thiel fluids. A vibrating actuator was used to generate phase change on the sample. Phase sensitive optical coherence tomography (PhS-OCT) was utilized to record the phase change of samples in a precise controlled time line, from which the time impact of quantitative Young's modulus was deduced. The technique presented in this paper has great potential application in the further development of fixatives for better maintenance of tissue properties. The results have significance on influencing fixative choice in biomedical instrument design.

2. Material and method

2.1 Sample preparation

To investigate the time impact of elasticity by formalin and Thiel fluids, five different tissue types were submerged into each fixative from fresh. The tissue types were porcine fat, porcine liver, chicken breast, chicken tendon and chicken cartilage. For each tissue type, 5 samples were prepared for the experiment. Random samples of chicken breast and porcine fat were taken with a 16-gauge biopsy needle. The chicken tendon samples were selected by directly dissecting a chicken drumstick. For the porcine liver and chicken cartilage, the random samples were cut and trimmed with a scalpel. The sample size was approximately 2mm in diameter and 1cm in length.

The two fixative solutions chosen were 10% formalin dilution and Thiel embalming fluids. Thiel embalming fluids are primarily salt based with boric acid and contain a very low concentration of formalin. The solution volume applied to each sample is ~30 ml. For the formalin treatment, the samples were immersed in 10% formalin dilution for 6 months. Thiel fluids utilised in this study are arterial infusion fluid, venous infusion fluid and tank fluid (Eisma et al., 2013) and the composition of each fluid is

demonstrated in Table 1. For the Thiel treatment, the samples were submerged in a mixture of 50/50 arterial and venous infusion fluids for 24 hours then transferred to tank fluid for the following 6 months. All fixation and experiments were conducted at room temperature.

TABLE 1. Composition of Thiel Embalming Fluids as Used in this study

	Arterial and Venous infusion (50/50) mixture	Tank fluid
Hot tap water [mL]	535.5	850
Boric acid [g]	16.35	24
Ammonium nitrate [g]	107.1	80
Potassium nitrate [g]	26.75	40
Sodium sulphite [g]	42.35	54
Glycol [mL]	159.55	80
Glycol/Chlorocresol mix [mL]	34.95	15
Formalin 37% [mL]	52.35	16
Morpholine [mL]	15.45	-
Alcohol [mL]	136.6	-
Total volume [mL] ca.	1000	1000

Imaging experiments were performed after 0, 10 minutes, 20 minutes, 30 minutes, 40 minutes, 50 minutes, and 1 hour, 70minues, 80 minutes, 90 minutes, 100minutes, 110 minutes, 2 hours, 3 hours, 4 hours, 5 hours, 6 hours, 7 hours, 8 hours, 9 hours, and 1 day, 2 days, 3 days, 4 days, 3 months, 6 months in the fixative.

During the OCE scanning, the tissue sample was taken out of the fixative and placed on 2% agar (mixed with 5% whole milk to produce a scattering background) with a thickness of ~10 mm which acted as an elasticity reference (Guan et al., 2013; Li et al., 2014). Each sample was scanned at the three clearly marked positions at each time interval. The scanning process took approximately 2 minutes per sample, dependent on the operator. The sample was kept moisture during the scan and returned to the fixative immediately after the procedure.

2.1 System configuration

The system setup has been described in previous reports (Li et al., 2014). The setup consists of two main parts: vibration stimulation and phase sensitive optical coherence tomography (PhS-OCT). In vibration stimulation, an electromagnetic actuator (Brüel & Kjær Sound & Vibration Measurement A/S) driven by a sine-wave modulated signal was used to produce vibration. The modulation frequency was set at ~8 kHz, and the maximum actuator displacement applied to the specimens was ~1 μm to ensure the generated strain was in pure linear-elastic regime. The vibration can then be transmitted from the actuator to compress the specimens and trigger vibration in the axial direction. Detection of the vibration signal was performed by a PhS-OCT system. The PhS-OCT system employs a superluminescent diode as a light source, with a centre wavelength of ~1310 nm and bandwidth of ~85 nm, implemented by a spectral domain configuration. The sample arm used an objective lens of ~30-mm focal length to deliver the detection light on the sample that coupled the vibration signals into the PhS-OCT for detection. The system provided an axial resolution of 8.9 μm and a transverse resolution of 15 μm in air. The acquisition rate was determined by the spectrometer employed in the system that had a maximum rate of ~76,000 A-scans/s. The dynamic range of the PhS-OCT system was measured to be ~100 dB at 0.5-mm axial depth with a phase noise of 3 mrad. However, the signal to noise ratio (SNR) in the region of interest (ROI) of the tissue sample was ~50 dB. For signal detection, the system was configured as M-mode acquisition while the OCT probe beam was constantly fixed in one location of the sample. The structural images of the samples generated by the PhS-OCT system were shown as a function of depth. For the acquisition of a cross-sectional two dimensional (2D) structural and elastography image, the OCT probe beam stayed for 512 repeat during A-line scan at every spatial location sequentially within the B-scan (total 512 locations) mode while the actuator repeatedly fired the stimulus. A complete B–scan consists of 512 × 512 A-scans. Synchronization of vibration generation and OCT beam scanning was precisely controlled using software written in the LabVIEW language.

The quantitative 2D stiffness of the sample was estimated from the data processing procedure previously described (Guan et al., 2013; Li et al., 2014). The vibration amplitude, related to the strain, is highly sensitive to the change of material elasticity. Under the same stress conditions, softer material has higher strain and stiffer material

has smaller strain. In vibrational OCE, the mechanical field is usually considered as a constant stress field, which means it is assumed that the same force is applied onto an area (Kennedy et al. 2013). Thus, under the same stress in a heterogeneous material, the ratio of Young's modulus in different regions is equal to the inverse ratio of the strain. Previous publications (Li et al., 2011; Li et al., 2012) proved that the Young's modulus of 2% agar phantom is known as ~193kPa. By the inversion method (Li et al., 2011; Li et al., 2012), the quantitative Young's modulus of the samples, which was placed on the agar phantom, can be estimated.

3. Results

3.1 The effect of formalin fixation to tissue elasticity

The two-dimensional elastography image with absolute Young's modulus values (Fig 1.) demonstrates the typical elasticity change of chicken breast which was fixed in 10% formalin dilution. The elasticity data was measured intensively at first, for the following hours then days and months within the strictly controlled timeline from 0 minute (control) to 3 days. The overall Young's modulus of specimen can be calculated from the elastograms. The Young's modulus was calculated by averaging Young's modulus value over the whole area associated. In addition, a clear tissue-air-agar boundary can be seen on the elasticity images, although the signal decreases at deeper locations. This is expected because the accuracy of the phase measurement relies on the intensity level from structure image (Guan et al., 2013).

As displayed Fig. 1, the elastograms were not taken from the identical detecting point on the chicken breast. However, the detection points were close to each other and no larger deviation needed to be considered. It can be clearly observed that the elasticity of formalin fixed chicken breast remained almost constant from the beginning of fixation to 100 minutes. A clear increase of tissue stiffness could be observed from 110 minutes of fixation. The stiffness increased slowly and tended to stabilise after approximately 1 day and remained constant afterwards. Note that different from other kinds of tissues which were relatively homogeneous in elastograms, fat tissue is heterogeneous in nature with hollows in the images. It is because only the stromal cells from porcine fat specimen, instead of transparent adipocyte, can be tracked by OCE.

The detailed time impact of elasticity change of fat, liver, muscle, cartilage and tendon by formalin fixation are compared in Fig. 2 and Fig, 3. Young's modulus of all tissue types increased due to the formalin fixation. However, each tissue type varied in time, speed and degree of fixation. Although the elasticity properties of soft tissues (chicken breast, porcine liver and fat) were similar before fixation, porcine liver had the lowest Young's modulus among them. After embedding them in the formalin for 6 months, the elasticity of porcine fat was even softer than porcine liver.

Porcine Fat

Formalin had the least effect on porcine fat, with overall increase by 54.7% from 280.7± 30.8 kPa to 434.2 ± 39.5 kPa. All other tissue types displayed a greater response to formalin fixation.

Chicken Breast

The Young's modulus of chicken breast increased significantly by 106.3% from 110 minutes' fixation from 244.7 ± 12.0 kPa to 504.9 ± 43.4 kPa. The majority increase occurred with the first 120 minutes. After 120 minutes, the Young's modulus of chicken breast raised slowly with fluctuations and reached approximately 645 kPa in 6 months of fixation. The overall rise of the Young's modulus of chicken breast induced by formalin was ~164%.

Chicken cartilage

The Young's modulus of chicken cartilage increased at a slower rate between 60-120 minutes' fixation (from 718.4 ± 63.2 kPa). The cartilage stiffness increased gradually until 4 hours where it reached its stability at ~1,100 kPa, with 58.7% overall increase.

Porcine liver

The elasticity changes in porcine liver were observed much earlier and occurred faster compared to all other tissue types. Changes in elasticity occurred within 20-30 minutes (from 249.7 ± 26.3 kPa) of formalin fixation and stabilised in approximately 50 minutes (to ~550 kPa) with overall increase of 120.2%.

Chicken Tendon

The Young's modulus of chicken tendon is much higher compared to other tissue types (Fig. 3). The initial value is 13,249.4 ±1,908.1 kPa. The increase in elasticity occurred between 120 minutes and 180 minutes and became stable at ~20,556.9 ± 1,779.3 kPa. The overall increase is 55.2%.

3.2 The effect of Thiel fixation to tissue elasticity

Figure 4 shows the elastograms taken from chicken breast specimens fixed with Thiel fluids within a strictly controlled timeline from 0 minute (control) to 3 days. The Thiel fixed samples show a different tissue response compared to formalin fixation. Chicken breast elasticity does not show any significant increase and remains almost constant from the beginning to the end of 3 days.

Figure 5 and figure 6 displays the time impact on the elasticity changes of fat, liver, muscle, cartilage and tendon by Thiel fluid fixation. In the first four days, the Young's modulus of all tissue types tends to remain stable during Thiel fluid fixation with small fluctuations compared to formalin fixation (Fig. 2 and Fig 3.). However, an increment of stiffness was observed from four days to 6 months. Among them, the porcine fat had a large increase of 72.5% from 211.9±43.5 kPa to 365.5±19.4 kPa.

4. Discussion and conclusion

Due to the limitation of the applied algorithm, the measured elasticity of the tissues is an approximate value acquired by comparing with the Young's modulus of the agar phantom, but this method is still capable to monitor the change of mechanical properties over time. Normally, Thiel cadavers are kept in a tank for at least 3-6 months before use, but the Thiel preserving time for smaller organs or tissue samples can be submersed for weeks. To replicate the fixation process, we investigated the elasticity change of the tissues embedded in formalin and Thiel solution for 6 months. No significant increase was observed in formalin samples, but the tissues in the Thiel solution tended to become stiffer after 3 months.

The data gathered displays an ascending trend in the elasticity changes for the samples immersed in 10% formalin dilution (Fig. 2 and Fig 3.). The samples immersed in Thiel solutions display constant values of Young's Modulus for all tissue types with only small fluctuations (Fig. 5 and Fig.6). As time elapsed, the formaldehyde penetrated into the tissue gradually, produced the cross-link of the proteins, and terminated any

ongoing biochemical reactions inside the tissue, leading to the augment of the tissue elasticity. 10% formalin solution has a much higher concentration of formaldehyde than Thiel solutions (Table 1.).

Since the size and density of the samples vary slightly, the distribution of Young's modulus is not uniform in some of the elasticity images, illustrated by the uneven colour (Fig 1.). There was very little change observed in the elasticity in the porcine fat sample. This may be as a result of there being fewer proteins within the tissue type for the formaldehyde to effect the protein structure as significantly as seen in other tissues.

The original elasticity of the tissues is slightly higher than that in the previous literature reports (Fig. 2-6). This could be attributed to the biochemical reactions and manual operation errors. Although the tissue was vacuum-packed before transferring to the OCE lab, there had been autolysis and decomposition to a certain extent. In addition, there was evaporation due to the ambient temperature change, especially on the surface of the tissue while preparing and scanning the sample. As a result, there might be some tissues partially dried out that could result in an increased level of stiffness.

When preparing the porcine liver sample, the process of cutting and trimming the sample took considerably longer (5 minutes) as the liver sample was too soft to handle. The preparation time for the chicken breast and porcine fat using a biopsy needle took less than a minute in comparison. The loss of moisture was minimised and well controlled in the other tissues, but relatively worse in the liver due to the nature of the tissue. As a result, the original value of elasticity of the liver was further increased and higher than literature reports (Chen et al., 2009; Frulio and Trillaud, 2013).

Theoretically, the tissue samples were ceased from further degradation by utilizing 10% formalin thus preserving functional cell and tissue structure, beneficial immunohistochemistry techniques. The combination of salts and glycol and reduced formalin in the Thiel solutions cease any further degradation of samples and provide a softer and flexible fixation than those fixed with formalin solution. However, it is difficult to stain Thiel nerves by standard H&E (Hematoxylin and Eosin stain) histological examination procedure due to the high concentration of salts in the Thiel fluids (Chandr).

In conclusion, this paper demonstrates that quantitative OCE method is suitable for monitoring elasticity changes during the fixation procedure of 10% formalin and Thiel

fluids. The elasticity changes of tissues in formalin solution display a rising trend, but changes in elasticity of Thiel fixed tissues are not obvious, likely to be as a result of the significantly reduced formalin concenetrations in Thiel solutions. The reduced changes in elasticity in Thiel fixed specimens help to retain lifelike textures and properties of tissues, enabling surgical and clinical training more approaching to the reality compared to traditional rigid formalin fixed specimens. This article demonstrates a novel technique that can be used to characterise and assess new fixation methods. Although there is no one fixative suitable for all the situations, there is potential using our structural images and elastograms to evaluate the time and concentration of the fixative required to produce specific tissue characteristics in the histopathology.

Acknowledgements

Authors thank Dr Paul Appleton, Dr Benjamin Cox and Professor Sandy Cochran for their assistant in this project.

References:

Abe M, Takahashi M, Horiuchi K and Nagano A 2003 The changes in crosslink contents in tissues after formalin fixation Anal. Biochem. 318 118–23.

Boskey A.L., Cohen M.L., Bullough P.G. 1982 Hard tissue biochemistry: a comparison of fresh-frozen and formalin-fixed tissue samples Calcified Tissue International, 34, pp. 328–331.

Buesa, R. J. and Peshkov M. V. 2012. "How much formalin is enough to fix tissues?" Ann Diagn Pathol 16(3): 202-209.

Chan R. C., Chau A. H., Karl W. C., Nadkarni S., Khalil A. S., Iftimia N., Shishkov M., Tearney G. J., Kaazempur-Mofrad M. R. and Bouma B. E., 2004 "OCT-based arterial elastography: robust estimation exploiting tissue biomechanics," Opt Express 12(19), 4558-4572.

Chandra A. "Study of damage to peripheral nerves caused by anaesthetic needles during regional anaesthesia." A thesis for the degree of MSc, University of Dundee.

Chen, S., et al. (2009). "Liver elasticity and viscosity quantification using shearwave dispersion ultrasound vibrometry (SDUV)." Conf Proc IEEE Eng Med Biol Soc 2009: 2252-2255.

Currey J.D., Brear K., Zioupos P., Reilly G.C. 1995 Effect of formaldehyde fixation on some mechanical properties of bovine bone Biomaterials, 16, pp. 1267–1271

D'Amico AV, Weinstein M, Li X, Richie JP, Fujimoto J. Optical coherence tomography as a method for identifying benign and malignant microscopic structures in the prostate gland. Urology. 2000;5:783–787.

Eisma, R., et al. 2013. From formalin to Thiel embalming: What changes? One anatomy department's experiences. Clin Anat 26(5): 564-571.

Eljamel, S, Volovick, A, Saliev, T, Eisma, R & Melzer, A 2014 Evaluation of Thiel cadaveric model for MRI-guided stereotactic procedures in neurosurgery Surgical Neurology International, 5(7): S404-S409.

Fercher A. F., 2010 "Optical coherence tomography - development, principles, applications," Z Med Phys 20(4), 251-276.

Frulio, N. and H. Trillaud (2013). "Ultrasound elastography in liver." Diagnostic and Interventional Imaging 94(5): 515-534.

Goh J.C., Ang E.J., K. 1989 Bose Effect of preservation medium on the mechanical properties of cat bones Acta Orthopaedica Scandinavica, 60, pp. 465–467.

Guan G, Li C, Ling Y, Vorstius JB, Keatch RP, Wang RK, Huang ZH; 2013 Quantitative evaluation of degenerated tendon model using combined optical coherence elastography and acoustic radiation force method. J. Biomed. Opt. 0001;18(11):111417-111417.

Kennedy B. F., Hillman T. R., McLaughlin R. A., Quirk B. C. and Sampson D. D., 2009 "In vivo dynamic optical coherence elastography using a ring actuator," Opt Express 17(24), 21762-21772.

Kennedy B. F., Liang X., Adie S. G., Gerstmann D. K., Quirk B. C., Boppart S. A. and Sampson D. D., 2011 "In vivo three-dimensional optical coherence elastography," Opt Express 19(7), 6623-6634.

Kennedy, K. M., et al. (2013). Analysis of mechanical contrast in optical coherence elastography. J Biomed Opt 18(12): 121508-121508.

Kikugawa, H. Asaka T. 2005 Effect of long-term formalin preservation on bending properties and fracture toghness of bovine compact bone Journal of the Japan Institute of Metals, 69, pp. 267–271.

Kirkpatrick S. J., Wang R. K. and Duncan D. D., 2006 "OCT-based elastography for large and small deformations," Opt Express 14(24), 11585-11597.

Ko H. J., Tan W., Stack R. and Boppart S. A., 2006 "Optical coherence elastography of engineered and developing tissue," Tissue Eng 12(1), 63-73.

Li C., Guan G., Reif R., Huang Z. and Wang R. K., 2011 "Determining elastic properties of skin by measuring surface waves from an impulse mechanical stimulus using phase-sensitive optical coherence tomography," Journal of The Royal Society Interface, doi: 10.1098/rsif.2011.0583.

Li C., Guan G., Cheng X., Huang Z., and Wang* R. K., 2012 "Quantitative elastography provided by surface acoustic waves measured by phase-sensitive optical coherence tomography", Optics Letters, 37 (4), pp. 722-724.

Li, C., Guan G., Ling Y., Hsu Y.T., Song S., Huang T. J. T., Lang S., Wang R. K., Huang Z., and Nabi G., 2014 Detection and characterisation of biopsy tissue using quantitative optical coherence elastography (OCE) in men with suspected prostate cancer, Cancer Letters , Volume 357 , Issue 1 , 121 – 128.

Liang X., Oldenburg A. L., Crecea V., Chaney E. J. andBoppart S. A. 2008, "Optical micro-scale mapping of dynamic biomechanical tissue properties," Opt Express 16(15), 11052-11065.

McLeod G, Eisma R, Schwab A, Corner G, Soames RW, Cochran S 2010 An evaluation of the Thiel cadaver for ultrasound based regional anaesthesia training and research. Ultrasound 18, 125-129.

McElhaney J., Fogle J., Byars E., Weaver G. 1964 Effect of embalming on the mechanical properties of beef bone Journal of Applied Physiology, 19, pp. 1234–1236.

Rogowska J., Patel N. A., Fujimoto J. G. and Brezinski M. E., 2004 "Optical coherence tomographic elastography technique for measuring deformation and strain of atherosclerotic tissues," Heart 90(5), 556-562.

Sedlin E.D. 1965 A rheologic model for cortical bone. A study of the physical properties of human femoral samples Acta Orthopaedica Scandinavica Supplementum, 83 (1965), pp. 77–81

Schmitt J. M., 1998 "OCT elastography: imaging microscopic deformation and strain of tissue," Opt Express 3, 199-211.

Tan C.I.C., Dunn S., Kent G.N., Randall A.G., Edmondston S.J., Singer K.P. 2002 Does formalin-fixation alter the extent of collagen and elastin crosslinks in human spinal intervertebral disks and ligamentum flava Journal of Muskuloskeletal Research, 6, pp. 89–99

Tearney GJ, Brezinski ME, Southern JF, Bouma BE, Boppart SA, Fujimoto JG. 1997 Optical biopsy in human urologic tissue using optical coherence tomography. J Urol.157:1915–1919.

Thiel, W. 2002. "Ergänzung für die Konservierung ganzer Leichen nach W. Thiel." Annals of Anatomy - Anatomischer Anzeiger 184(3): 267-269.

Tomlins P. H. and Wang R. K., 2005 "Theory, developments and applications of optical coherence tomography," Journal of Physics D: Applied Physics 38(15), 2519-2535.

Wang R. K., Kirkpatrick S. andHinds M., 2007 "Phase-sensitive optical coherence elastography for mapping tissue microstrains in real time," Appl Phys Lett 90(16), 164105-164103.

Wang R. K. K., Ma Z. H. and Kirkpatrick S. J., 2006 "Tissue Doppler optical coherence elastography for real time strain rate and strain mapping of soft tissue," Appl Phys Lett 89(14), 144103.

Wang R.K, Nuttall AL. Phase-sensitive optical coherence tomography imaging of the tissue motion within the organ of Corti at a subnanometer scale: a preliminary study. Journal of Biomedical Optics. 2010;15(5):056005. doi:10.1117/1.3486543.

Welzel, J. 2001 "Optical coherence tomography in dermatology: a review," Skin Res Technol 7(1), 1-9.
Sun C., Standish B. and Yang V. X. D., 2011 "Optical coherence elastography: current status and future applications", J. Biomed. Opt. 16, 043001.

Wolff, K. D., et al. 2008. Thiel embalming technique: a valuable method for microvascular exercise and teaching of flap raising. Microsurgery 28(4): 273-278.

Figures:

Figure 1. Typical elasticity change of 10% formalin dilution fixed chicken breast with precisely controlled time line.

Figure 2. Elasticity change of fat, liver muscle and cartilage induced by formalin.

Figure 3. Elasticity change of tendon induced by formalin.

Figure 4. Typical elasticity change of Thiel fluid fixed chicken breast within a precisely controlled time line.

Figure 5 Elasticity change of fat, liver muscle and cartilage induced by Thiel fluid.

Figure 6 Elasticity change of tendon induced by Thiel fluid.

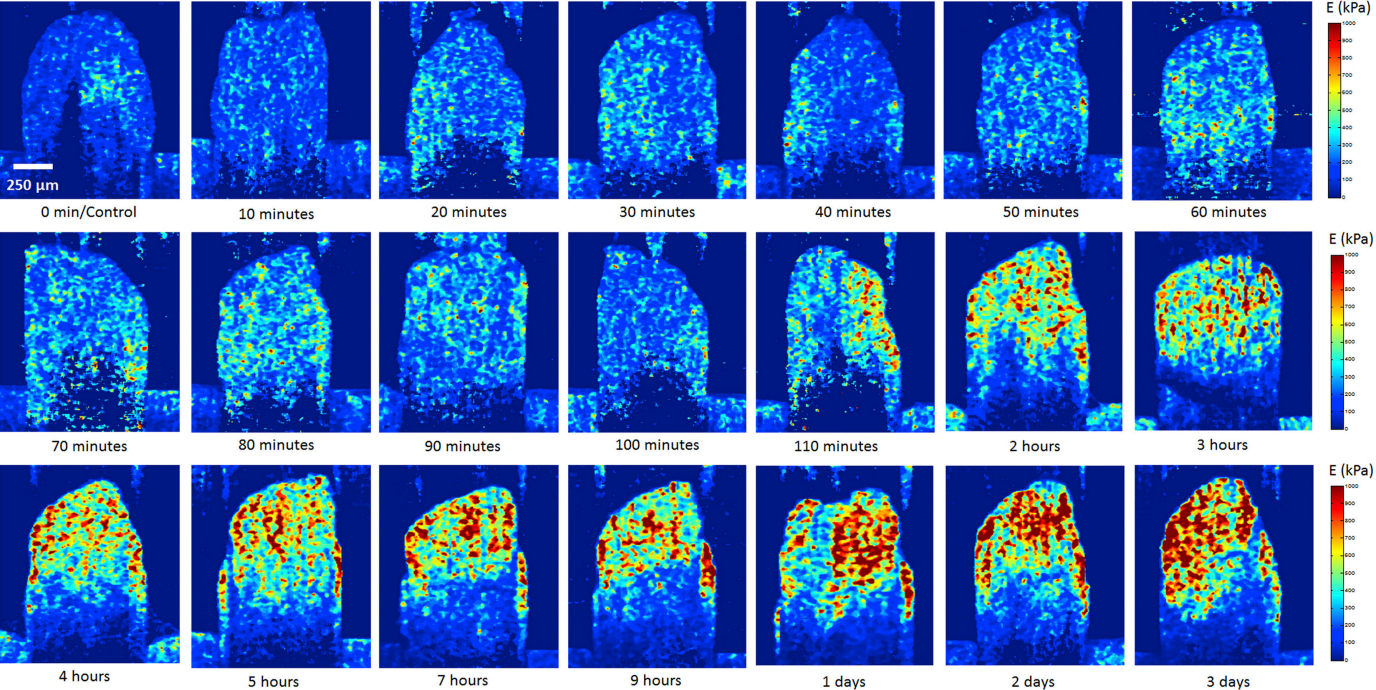
250 µm
E (kPa)
1000
900
800
700
600
500
400
300
200
100
0
0 min/Control
10 minutes
20 minutes
30 minutes
40 minutes
50 minutes
60 minutes
70 minutes
80 minutes
90 minutes
100 minutes
110 minutes
2 hours
3 hours
4 hours
5 hours
7 hours
9 hours
1 days
2 days
3 days

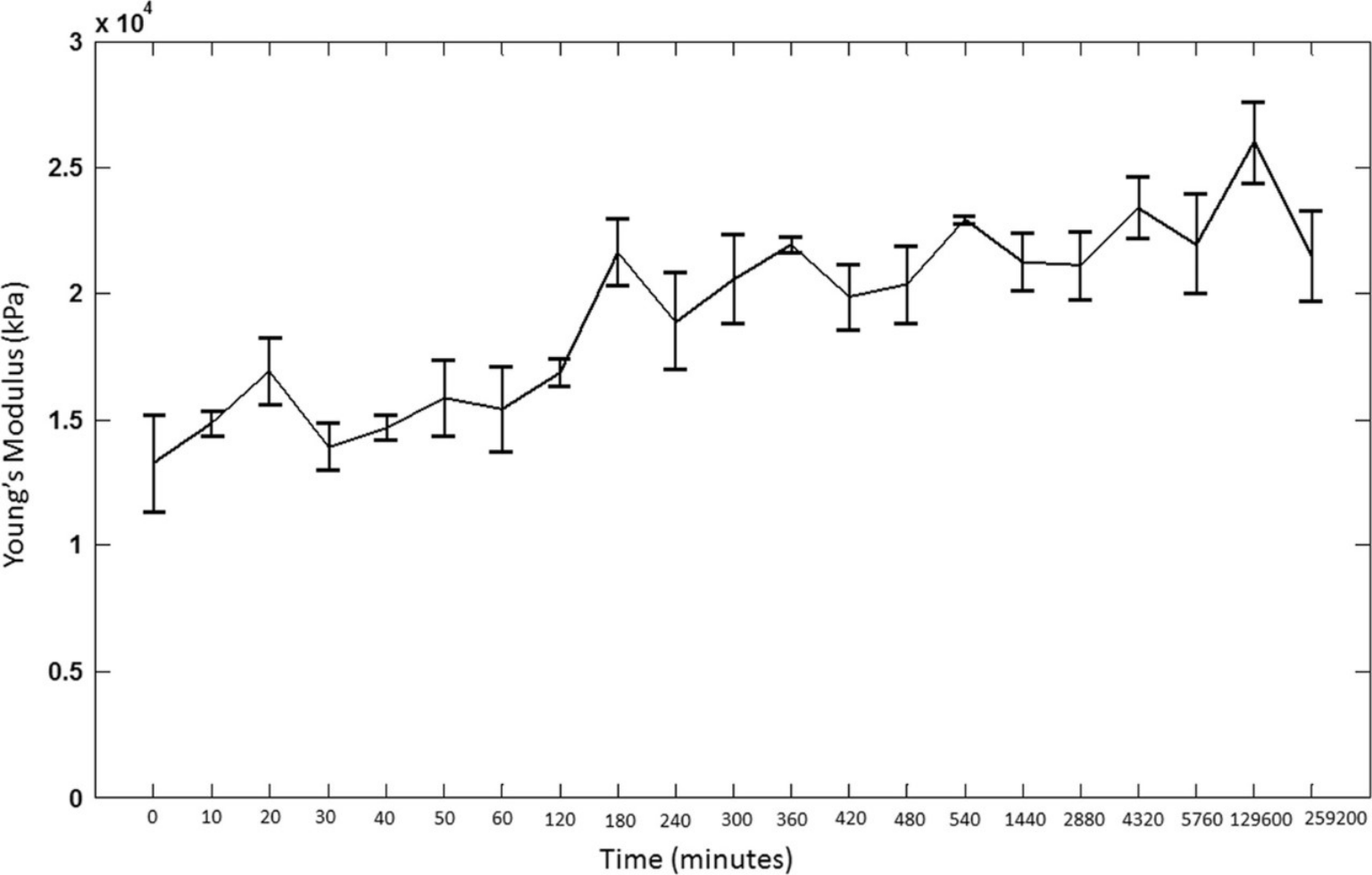
x 10^4
3
2.5
2
1.5
1
0.5
0
Young's Modulus (kPa)
0
10
20
30
40
50
60
120
180
240
300
360
420
480
540
1440
2880
4320
5760
129600
259200
Time (minutes)

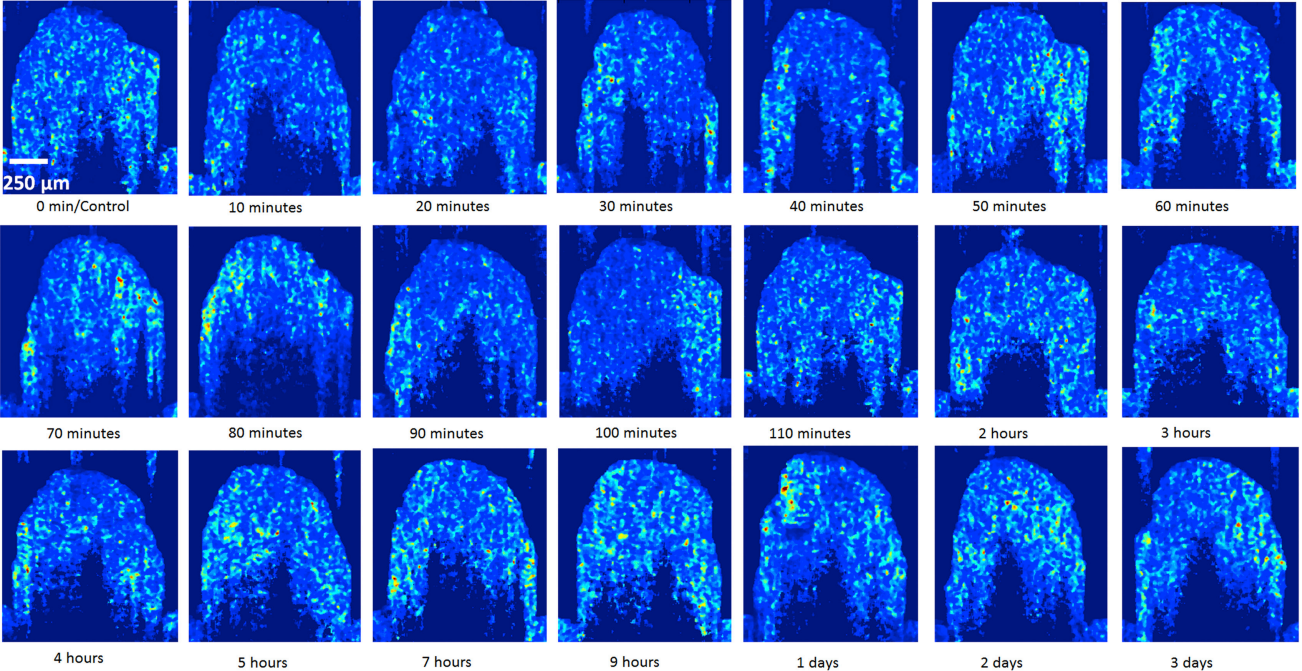
250 µm
0 min/Control
10 minutes
20 minutes
30 minutes
40 minutes
50 minutes
60 minutes
70 minutes
80 minutes
90 minutes
100 minutes
110 minutes
2 hours
3 hours
4 hours
5 hours
7 hours
9 hours
1 days
2 days
3 days
E (kPa)
1000
900
800
700
600
500
400
300
200
100
0

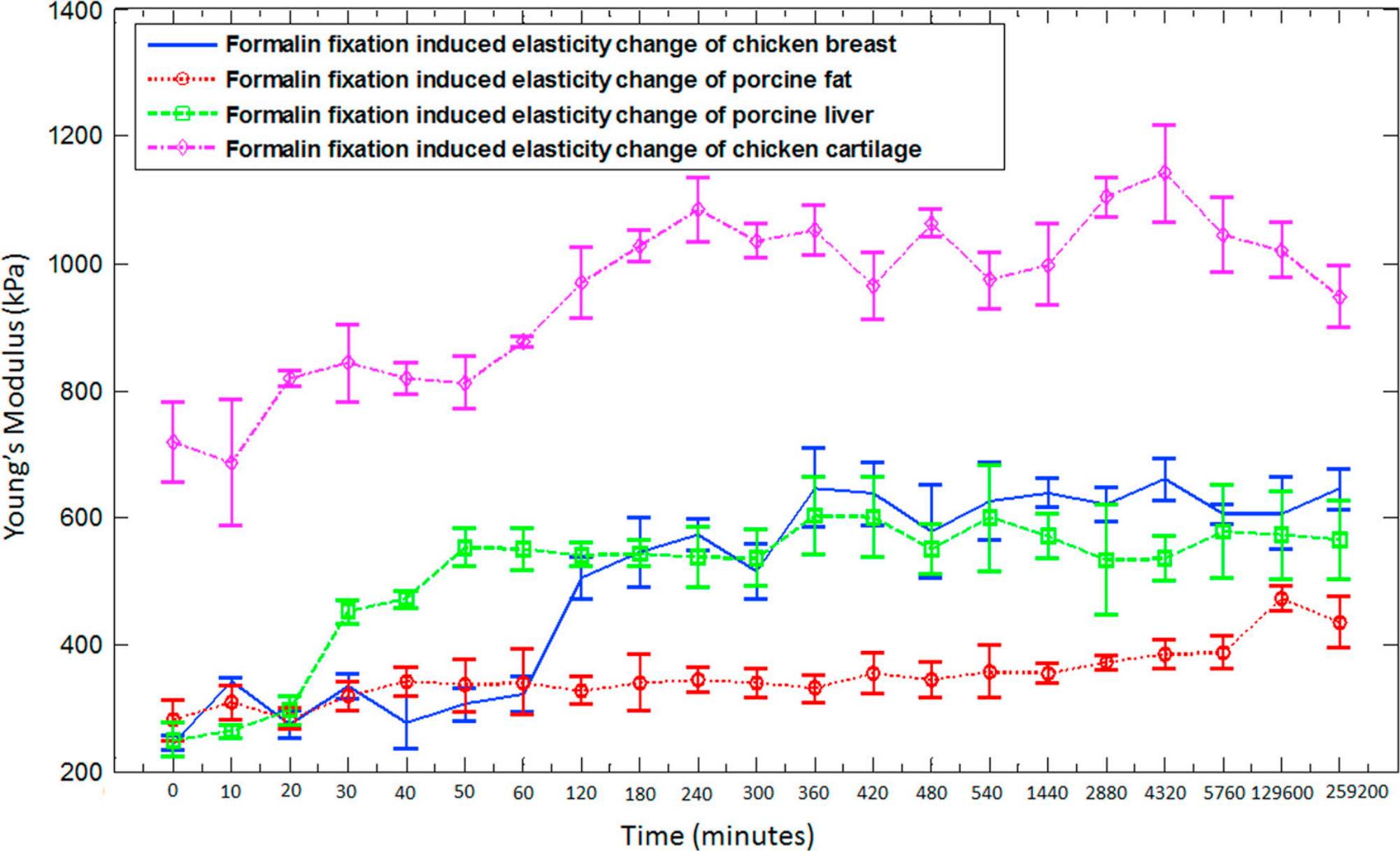
Formalin fixation induced elasticity change of chicken breast
Formalin fixation induced elasticity change of porcine fat
Formalin fixation induced elasticity change of porcine liver
Formalin fixation induced elasticity change of chicken cartilage
Young's Modulus (kPa)
1400
1200
1000
800
600
400
200
0
10
20
30
40
50
60
120
180
240
300
360
420
480
540
1440
2880
4320
5760
129600
259200
Time (minutes)

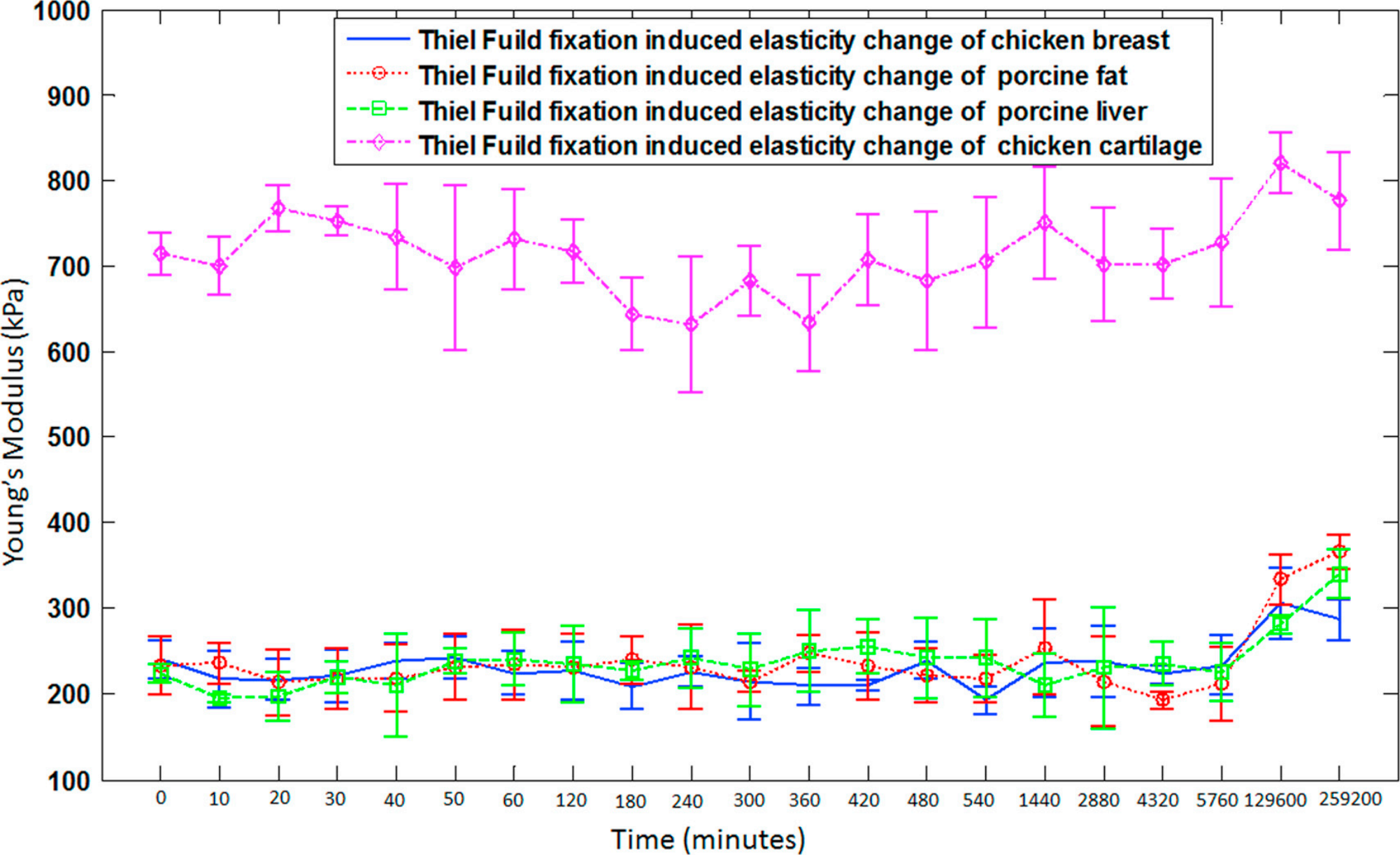
Thiel Fuild fixation induced elasticity change of chicken breast
Thiel Fuild fixation induced elasticity change of porcine fat
Thiel Fuild fixation induced elasticity change of porcine liver
Thiel Fuild fixation induced elasticity change of chicken cartilage
Young's Modulus (kPa)
1000
900
800
700
600
500
400
300
200
100
0
10
20
30
40
50
60
120
180
240
300
360
420
480
540
1440
2880
4320
5760
129600
259200
Time (minutes)

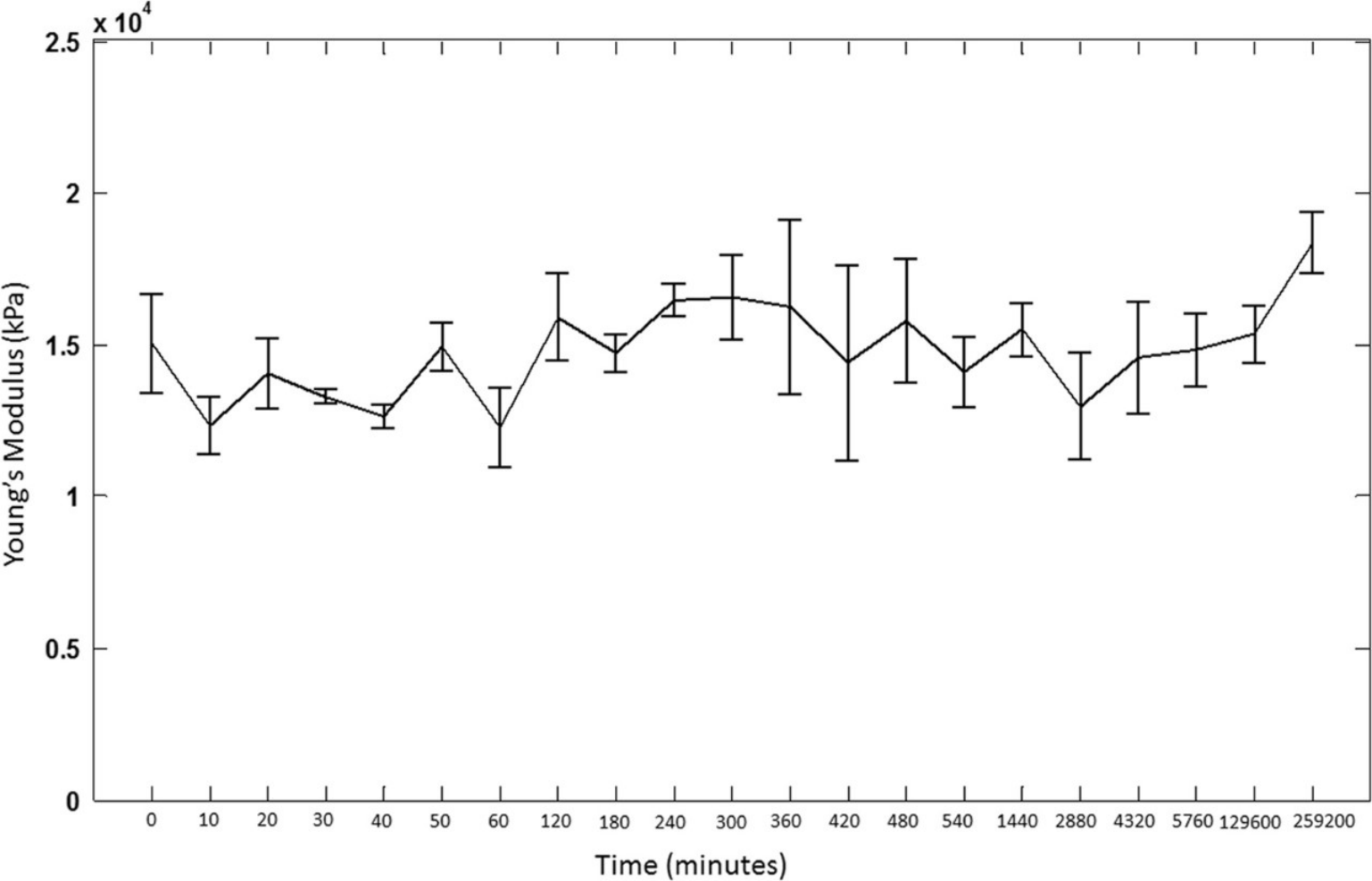
x 10^4
2.5
2
1.5
1
0.5
0
Young's Modulus (kPa)
0
10
20
30
40
50
60
120
180
240
300
360
420
480
540
1440
2880
4320
5760
129600
259200
Time (minutes)

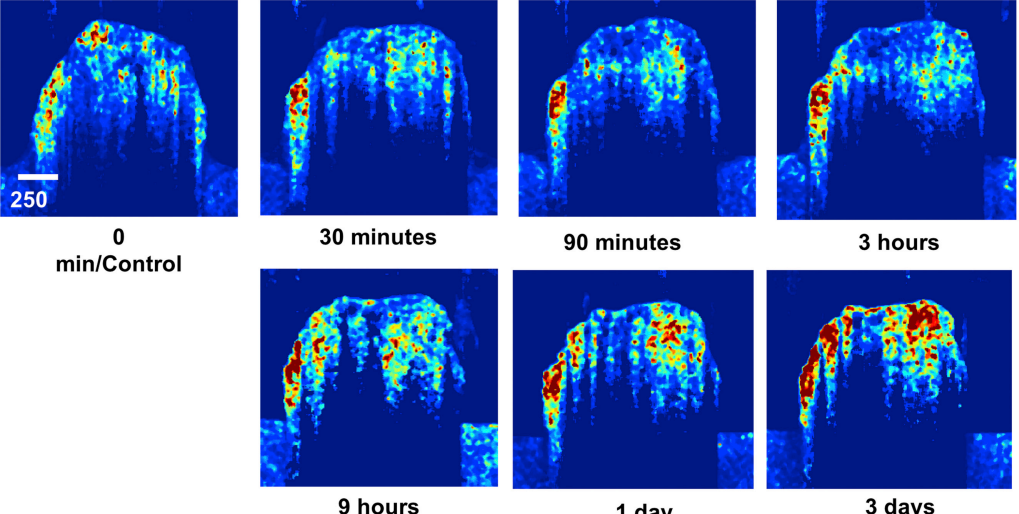
E (kPa)
1000
900
800
700
600
500
400
300
200
100
0
250
0
min/Control
30 minutes
90 minutes
3 hours
9 hours
1 day
3 days